MAUSAM, **75**, 1 (January 2024), 181-190

MAUSAM

DOI : https://doi.org/10.54302/mausam.v75i1.6081
Homepage: https://mausamjournal.imd.gov.in/index.php/MAUSAM

UDC No. 551.577.37 : 551.524 : 551.509.314 (540.17)

Future projections of precipitation and temperature extremes at Sohra (Cherrapunji) using Statistical Downscaling Model

RAJU KALITA, DIPANGKAR KALITA and ATUL SAXENA

Department of Physics, North-Eastern Hill University, Shillong, India

(*Received 21 November 2022, Accepted 23 November 2023*)

e mail : kalita.raju.nehu@gmail.com

सार – **सांख्यिकीय डाउनस्केलिंग मॉडल** (SDSM 4.2) **का उपयोग दूसरी पीढ़ी के कनाडा के पृथ्वी प्रणाली मॉडल** (CanESM2) **के पूर्वानुमानकर्त्ताओं का उपयोग करते हुए, सोहरा में वर्षा और अधिकतम तथा न्यूनतम तापमान का अनुमान लगाने के लिए किया जाता है, जो पृथ्वी पर प्रचण्ड घटनाओं के स्थानों में से एक है। एसडीएसएम का आशांकन** 1979 **से** 2005 **तक के दैनिक वर्षा और तापमान से किया गया और** 2006 **से** 2020 **तक डेटा के साथ इसे वैधीकृत किया गया। तीन महत्वपूर्ण सांद्रता पथ** (RCP) 2.6, 4.5 **और** 8.5 **के तहत उत्पन्न भविष्य के परिदृश्यों को भविष्य की तीन अवधियों में विभाजित किया गया जैसे निकट भविष्य** (2021-2040) **मध्य भविष्य** (2041-2071), **और सुदूर भविष्य** (2071-2100)**। यह पाया गया है कि सोहरा में वर्षा और अधिकतम/न्यूनतम तापमान मुख्य रूप से प्रमुख वैश्विक अनुमानकर्ता क्रमश:** 850 **एचपीए ऊंचाई (एस**850) **पर विशिष्ट आर्द्रता,** 2 **मीटर (तापमान)/सतह विशिष्ट आर्द्रता औसत तापमान से प्रभावित होते हैं। डाउनस्केल्ड परिणाम से ज्ञात होता है कि निकट भविष्य के दौरान आधार अवधि** 1985-2005 **और मध्य और सुदूर भविष्य के दौरान** 1979-2008 **की तुलना में विभिन्न आरसीपी के तहत मॉनसून वर्षा में** 266-1543 **मिमी तक की वृद्धि हुई है। साथ ही, भविष्य में सभी आरसीपी के लिए वार्षिक अधिकतम और न्यूनतम तापमान में** 1-2.8 **डिग्री सेल्सियस और** 1.2-3.6 **डिग्री सेल्सियस की वृद्धि होगी।**

ABSTRACT. The Statistical Downscaling Model (SDSM 4.2) is used to project the future precipitation and maximum and minimum temperatures at Sohra, one of the extreme places on earth, using the predictors of the Second-Generation Canadian Earth System Model (CanESM2). The SDSM was calibrated with daily precipitation and temperature data from 1979 to 2005 and validated from 2006 to 2020. Future scenarios generated under the three Representative Concentration Pathways (RCP) 2.6, 4.5 and 8.5 are divided into three future periods, Near Future (2021-2040), Mid Future (2041-2071), and Far Future (2071-2100). It is found that the precipitation and maximum/minimum temperature at Sohra are influenced mainly by the major global predictors; specific humidity at 850 hPa height (s850) and mean temperature at 2 m (temp)/near surface specific humidity (shum), respectively. The downscaled result reveals an increase in Monsoon precipitation in the range of 266-1543 mm under various RCPs compared with the base periods 1985-2005 during the Near Future and 1979-2008 during the Mid and Far Future. Also, annual maximum and minimum temperature increases in the range of 1-2.8 °C and 1.2-3.6 °C for all RCPs in the future.

Key words – SDSM, Precipitation, Temperature, Sohra, Future projection, CanESM2.

1. Introduction

Anthropogenic activities have led the climate of the globe to change much faster than before, as reported by the IPCC 6th assessment report (IPCC, 2021). Consequently, there is a likelihood of an increase in extreme events like floods, drought, heat waves, etc., on the local scale. These extreme events could impact the livelihood of society, human health, agriculture, urban development, water availability and many more aspects of life. To cope with such circumstances, it is essential to understand the future state of the climate with the available historical climate information. For this, climate projections are made using the Global Climate Model or General Circulation Model (GCM) at a coarse resolution. GCMs are often reliable in global scale projections with large grid sizes up to the order of 50,000 sq km (Wilby *et al.*, 2002). However, due to coarser resolution, unresolved microscale processes, terrain difference, and convections, it can rarely project at regional or local scale,

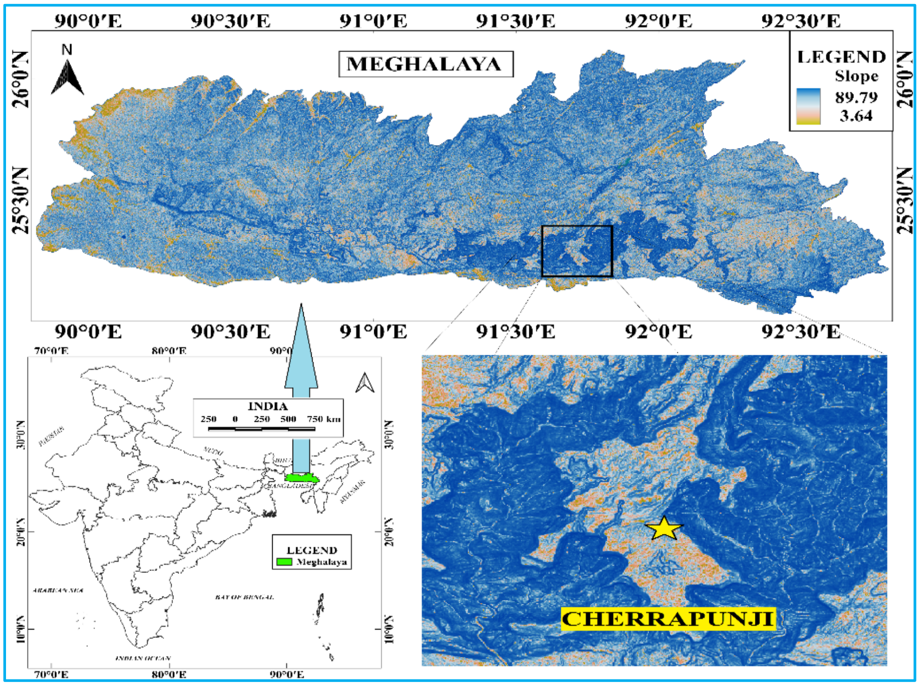

Fig. 1. Study Location of Sohra (Cherrapunji)

as accurately as at large scale. In fact, higher uncertainties are associated with complex mountainous topography having extreme climatic conditions. Using downscaling techniques, projections at local level or site level is possible and are quite popular tools among climatologists and hydrologists nowadays. Basically, downscaling can be achieved by two approaches, Dynamical Downscaling (DD) and Statistical Downscaling (SD). In DD, a Regional Climate Model (RCM) of finer resolution is forced or nested within a GCM to produce outputs at regional level. While in SD, the relationship established between the large-scale global predictors and local scale predictands is downscaled empirically or statistically. Both methods are comprehensive and give promising result. DD is based on physical processes and requires high computations. However, SD is quite handy, computationally inexpensive, and based on statistics. The efficiency in SD depends on how accurately the model is calibrated with the appropriate choice of predictors, which can significantly influence the predictands at the regional level. Moreover, the length of observed and historical data and the choice of regression process also affect the model efficiency. In general, SD is faster and is a good alternative to assess climate impact analysis, hydrological responses to various climate scenarios, and to downscale important climate variables such as precipitation, temperature, evapotranspiration, *etc*. The downscaling of identically independent and conditional events like precipitation is difficult compared to unconditional events like temperature. Due to nonlinearity and high spatial and temporal variability, statistical downscaling of precipitation could rarely show high efficiency (Maraun *et al.*, 2010).

The Statistical Downscaling Model (SDSM) is one of the most widely used downscaling approaches to assess climate change and climate impact analysis at the regional level (Sharma *et al.*, 2007; Akhtar *et al.*, 2008; Elshamy *et al.*, 2009; Wetterhall *et al.*, 2009; Huang *et al.*, 2011; Kannan and Ghosh, 2011; Souvignet and Heinrich 2011). To date, various studies have been carried out in the South Asian region using both Statistical, and Dynamical Downscaling approaches (Tripathi *et al.*, 2006; Anandhi *et al.*, 2007; Akhtar *et al.*, 2008; Ghosh and Mujumdar, 2008; Ashiq *et al.*, 2010; Goyal and Ojha, 2010; Mahmood and Babel, 2013; Shafiq *et al.*, 2019). In the Indian context, the precipitation is primarily due to summer rainfall, which contributes to about 80 % of the annual precipitation in India (Bollasina, 2014). Most of the studies using GCMs suggest that the Indian monsoon rainfall will increase due to climate change in the 21st century (Chaturvedi *et al.*, 2012; Menon *et al.*, 2013; Lee and Wang, 2014; Asharaf and Ahrens, 2015; Mei *et al.*, 2015; Sharmila *et al.*, 2015; Varghese *et al.*, 2020). Whereas the mean surface temperature is likely to increase, and the warming across the country may vary at a different rate by the end of the 21st century (Kumar *et al.*, 2013; Basha *et al.*, 2017; Das and Umamahesh,

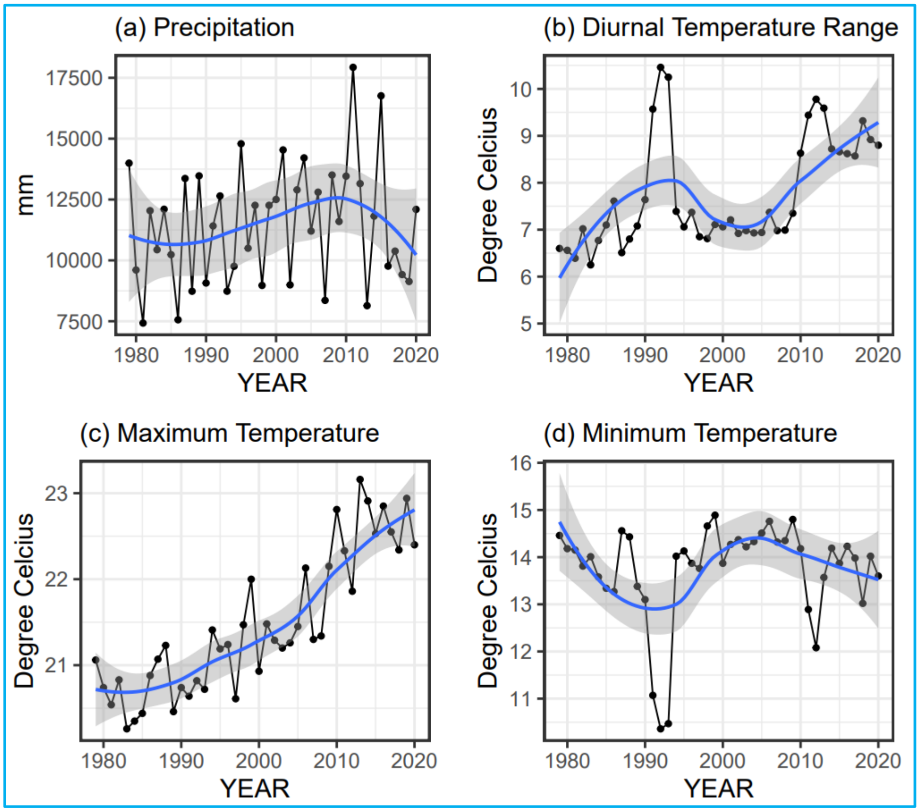

Figs. 2(a-d). Observed mean annual (a) precipitation, (b) diurnal temperature range, (c) maximum temperature and (d) minimum temperature at Sohra from 1979 to 2020

2022). Under Representative Concentration Pathway 8.5 (RCP 8.5), CMIP5 models project a median increase in Indian monsoon rainfall of 2.3% per Kelvin rise in temperature (Menon *et al.*, 2013). Also, under RCP 8.5, the amount of rainfall over India is projected to increase by 18.7 % towards the end of the 21st century compared to 1961-1999 (Chaturvedi *et al.*, 2012). The same study showed that the mean warming in India is likely to be in the range of 1.7-2 °C by 2030s and 3.3-4.8 °C by 2080s relative to the preindustrial time scenario between RCP 6.0 and RCP 8.5. Moreover, the increase in maximum temperature anomaly is likely to cause severe heat wave events in the regions of southern, northeast, and western parts of India (Das and Umamahesh, 2022). Some models even project that the increase will contribute to precipitation, especially in the Himalayan region, northeast of the Bay of Bengal and the west coast of India (Gusain *et al.*, 2020). Though North-Eastern Indian rainfall is trendless, some studies predicted that the daily mean rainfall would likely to increase in the future (Salvi and Ghosh, 2013). Due to unique topography and orographic features, the North-Eastern region of India receives the highest annual rainfall compared to the rest of India. Furthermore, Sohra (Cherrapunji) is among such places with extreme precipitation and the highest recorded one day rainfall in a calendar month. Hence, in this study, we aim to downscale the precipitation as well as the maximum and minimum temperature of Sohra from the CanESM2 outputs to observe their variability in the future under three emission scenarios, RCP 2.6, 4.5 and 8.5, respectively.

2. Study area, data and methodology

2.1. *Study Location and its Climate*

Sohra (Cherrapunji) is located at the Southern edge of stiff mountainous cliffs of the Hilly State of Meghalaya in North-Eastern India and is at an altitude of about 4823 feet (1484 m) above the mean sea level (Fig. 1). It acts as a first orographic barrier for the westerly wind, which carries the moist and warm air over the Bay of Bengal and is responsible for the heavy monsoon in Sohra. The average temperature is moderate and ranges between 11.6 °C during January (Winter) to 20.6 °C during August (Summer), respectively.

TABLE 1

List of Screened out predictors used for the calibration

Predictand	Rank	Predictors	Description	R1 (%)	PRP (%)	P value
Precipitation	1	nceps850	Specific humidity at 850 hPa height	37.6	SP	0
	2	ncepp850	850 hPa geopotential height	31.8	83.9623	0
	3	ncepp500	500 hPa geopotential height	26.4	84.4697	0
	4	ncepmslp	Mean sea level pressure	33.8	82.2485	0
Maximum Temperature	1	nceptemp	Mean temperature at 2 m	61.3	SP	0
	2	ncepp5_z	500 hPa vorticity	36	76.1111	0
	3	ncepp500	500 hPa geopotential height	58.5	50.7692	0
	4	ncepmslp	Mean sea level pressure	43.8	73.7443	0
Minimum Temperature	1	ncepshum	Near surface specific humidity	84.2	SP	0
	2	ncepp500	500 hPa geopotential height	74.2	82.6146	0
	3	nceps850	Specific humidity at 850 hPa height	83.2	86.7788	0
	4	ncepp850	850 hPa geopotential height	56	79.1071	0

2.2. *Data used*

The observed daily precipitation, maximum temperature (*T*max) and minimum temperature (*T*min) data (1979-2020) used for calibration and validation of SDSM was obtained from the website of Cherrapunjee Holiday Resort which keeps the daily data that is collected from the meteorological station of the Indian Meteorology Department at Sohra. While, the historical NCEP-NCAR (National Center of Environmental Prediction-National Center for Atmospheric Research) climate data and future climate scenario data of 26 predictors for RCP 2.6, 4.5, and 8.5 were obtained from the second-generation Canadian Earth System Model with appropriate grid box for Sohra [CanESM2 predictors: CMIP5 experiments (Canada.ca)].

2.3. *Statistical downscaling model*

SDSM is a hybrid of multiple linear regression (MLR) and the stochastic weather generator (SWG) developed by Wilby *et al.*, (2002). It is a window-based decision support tool coded in Visual Basic 6.0 and is the first of its kind offered to the broader climate change impacts community. The model uses MLR techniques to establish relationships between the NCEP, historical large-scale circulation pattern, atmospheric variables (predictors) and local scale variables (predictands) and produces some regression parameters. SWG uses the NCEP and GCM predictors along with these calibrated regression parameters to simulate an ensemble of 20-100 daily time series to correlate better with the observed time series. The model can develop a low-cost, single-site, ensemble scenario of daily surface weather variables under present and future climate forcing using seven key functions; (*i*) quality control and data transformation, (*ii*) screening of predictor variables, (*iii*) model calibration, (*iv*) weather generation, (*v*) statistical analysis, (*vi*) graphing model output and (*vii*) scenario generation.

3. Result and discussion

3.1. *Characteristics of observed Precipitation and Temperature*

Analysis of observed mean annual temperature (maximum and minimum), precipitation, and diurnal temperature range (DTR) is carried out for Sohra from 1979 to 2020 using Mann Kendall trend test and Sen's Slope estimator to determine the trend and magnitude of that trend. It was observed that only DTR and maximum temperature showed a significant increasing trend at 99% significant level with 0.05 and 0.06 °C/year, respectively [Figs. 2(b&c)]. Precipitation and minimum temperature did not show any significant trend [Figs. 2(a&d)]. Also, the summary statistics revealed that Sohra witnessed 11,477 mm of mean annual rainfall in the range of 7,424-17,930 (min-max) mm. Moreover, the mean annual DTR, *T*max and *T*min were 7.7, 21.5 and 13.7 °C, respectively.

3.2. *Screening of predictors*

The selection of appropriate predictors is the central task of downscaling by SDSM. Out of 26 global predictors of CanESM2, only a few which showed a

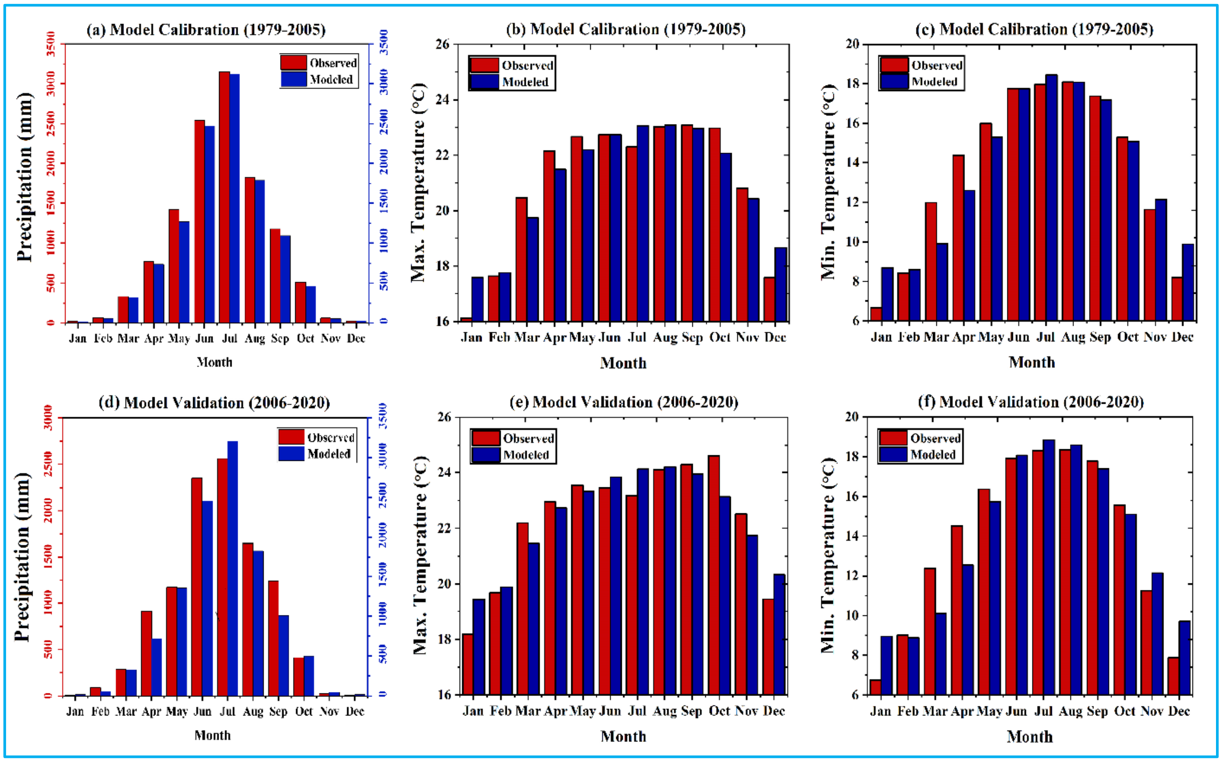

Figs. 3(a-f). Model performance during Calibration and Validation of monthly precipitation (a, d), monthly maximum temperature (b, e) and monthly minimum temperature (c, f)

significant relationship with the local scale predictands were chosen for calibrating and downscaling the model. To screen out the relevant predictors, a combination of the correlation matrix, partial correlation, and *P* value at 0.05 significance level is used, as described by Mahmood and Babel (2013). The predictor with the highest correlation coefficient among all predictors is selected as a super predictor (SP), and then, the percentage reduction in an absolute partial correlation (PRP) with respect to absolute correlation is calculated for the rest of the predictors which using the following equation:

$$\text{PRP} = \left(\frac{P.r - R1}{R1}\right) \tag{1}$$

where $P.r$ is the partial correlation coefficient and $R1$ is the correlation coefficient between predictor and predictand. Thus, four predictors are screened out, one super predictor and three with a minimum PRP value (Table 1). It was observed that Specific humidity at 850 hPa (nceps850), Mean temperature at 2 m (nceptemp), and Near surface specific humidity (ncepshum) were found to be the SPs for precipitation, *T*max, and *T*min at Sohra, respectively. Most of the selected predictors are in agreement with similar studies over the Himalayan region (Khadka and Pathak, 2016; Shafiq *et al.*, 2019).

3.3. *Calibration and validation*

Calibration is an essential step that involves the establishment of a regression relationship between the screened-out predictors from CanESM2 and the local scale predictands. The predictors listed in Table 1 were used for the calibration of SDSM. Also, the reliability of the calibrated model was validated with the simulated results during the observation period. Thus, the daily weather data series was divided into two sets. Data sets from 1979 to 2005 were used for calibration, while the rest from 2006 to 2020 were used for validation for each of the predictands. During the simulations, the model was set to conditional process for precipitation and unconditional for temperature. Fig. 3 shows the month-wise comparison of observed and modeled predictands for precipitation, maximum temperature, and minimum temperature during both the calibration [Figs. 3(a-c)] and validation [Figs. 3(d-f)] period.

A statistical index, Correlation Coefficient (R), was used to assess the model performance for the predictands during the period of observation. In the calibration period,

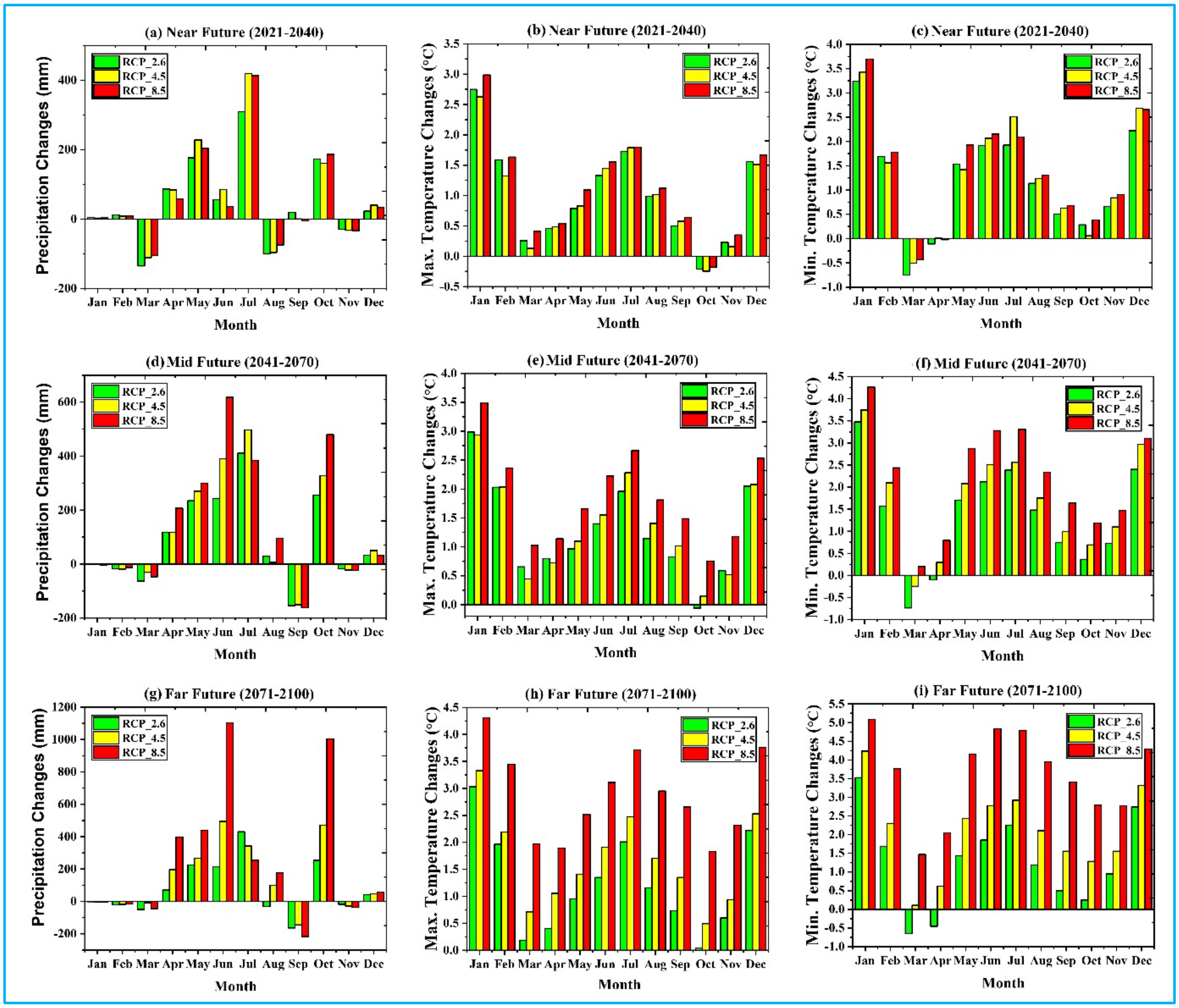

Figs. 4(a-i). Projected changes in monthly precipitation, monthly maximum temperature, and monthly minimum temperature during the future periods 2021-2040 (a-c), 2041-2070 (d-f), and 2071-2100 (g-i), respectively

R for precipitation was found to be 0.99, whereas *T*max and *T*min were found to be 0.96 for both. Similarly, the validation period gave *R* values of 0.99, 0.93, and 0.95 for the precipitation, *T*max, and *T*min, respectively. It is often difficult to simulate daily precipitation due to its heterogeneous nature, and therefore, it is poorly resolved by the large-scale predictors compared to daily temperature. However, in this study, the Correlation Coefficient values suggest a better simulation of precipitation and temperature variables.

3.4. *Future projection*

With the calibrated model, future scenarios were generated for the predictands under the Representative Concentration Pathways (RCP) 2.6, 4.5 and 8.5 from the outputs of CanESM2 for Near Future (2021-2040), Mid Future (2041-2070) and Far Future (2071-2100) periods. It is to mention here that the results were generated using the mean of 20 ensembles of the downscaled scenarios. The projected results were compared with the base period 1986-2005 for NF and 1979-2008 for both MF and FF, respectively, shown in Fig. 4. Also, the seasonal projections were compared for four seasons; Winter (Jan-Feb), Pre-Monsoon (Mar-May), Monsoon (Jun-Sep) and Post-monsoon (Oct-Dec).

3.4.1. *Precipitation*

The generated scenario reveals that the average monthly precipitation will increase sufficiently from Apr to Jul and in Oct in the three future periods for all RCPs

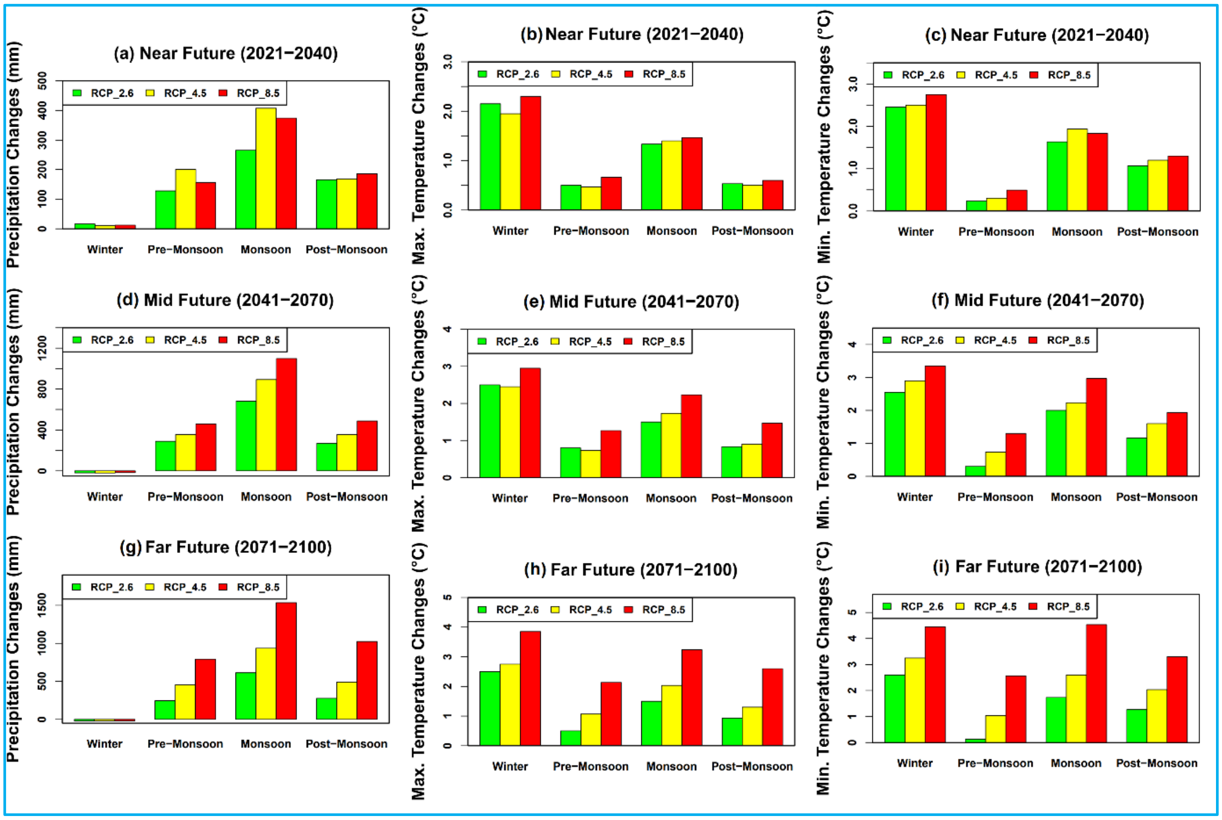

Figs. 5(a-i). Projected changes in seasonal precipitation, seasonal maximum temperature, and seasonal minimum temperature during the future periods 2021-2040 (a-c), 2041-2070 (d-f), and 2071-2100 (g-i), respectively

[Figs. 4(a, d&g)]. In contrast, decrement in precipitation will be observed for Mar and Aug of the Near Future (NF) and Sep of Mid Future (MF) and Far Future (FF) periods in all three scenarios. However, little changes will be observed in Jan, Feb, Nov, and Dec months for all RCPs in the future. The month of July will witness a maximum increment (310-420 mm) in precipitation by all the RCPs during NF, by RCP 2.6 (410 mm) and 4.5 (496 mm) during MF, and only by RCP 2.6 (430 mm) during FF. However, in the case of RCP 8.5 of Mid Future (618 mm) and Far Future (1103 mm), and RCP 4.5 of FF (494 mm), the maximum increment in precipitation will be observed for June month. It is observed that with higher RCPs, the maximum change will be shifted from July to June in the future.

The projected change in seasonal precipitation at Sohra shows that it will increase though out all the seasons in the three future periods except during the Winters of MF and FF [Figs. 5(a, d&g)]. The maximum increase in precipitation will be observed during the Monsoon for all the RCPs, followed by the pre-monsoon and post-monsoon seasons. However, little change will be observed during winter. For the monsoon season, the precipitation increment will vary from 266 mm during NF for RCP 2.6 to 1543 mm during FF for RCP 8.5. While, in pre- and post-monsoon, the increment will vary from 128 and 163 mm during NF for RCP 2.6 to 792 and 1024 mm during FF for RCP 8.5, respectively. Also, with higher RCPs, the change in seasonal precipitation increases during MF and FF.

3.4.2. *Maximum temperature*

The downscaled results for the three RCP show that the projected maximum temperature will increase every month throughout the year in future periods, except for Oct of NF in all RCPs and the Oct of MF in RCP 2.6 only [Figs. 4(b, e&h)]. The annual maximum temperature increases by 1-1.1 °C during NF, 1.2-1.8 °C for MF and 1.2-2.8 °C during FF. The highest change in maximum temperature is shown by January month (2.6-4.3 °C) in all the three RCPs during the entire future periods. Also, Feb and Dec show a relatively higher increase in *T*max as compared to other months, excluding Jan. Also, the worst scenario is shown by the RCP 8.5, as it shows a higher increment in *T*max for the RCP 2.6 and RCP 4.5 of MF and FF, respectively. It is observed that the change in maximum temperature increases from Mar, reaches a peak during July, and then decreases till Sep. Again, it starts rising from Oct, peaks during Jan and goes down till Mar. This indicates that the summer and winter months will be most affected in the future as the increase in daytime temperature is much higher relative to the other months.

Also, seasonal projections show an increase in *T*max for the three RCP in the future [Figs. 5(b, e&h)]. The maximum increase is projected for Winters, followed by Monsoon for all the RCPs during the future periods. For RCP 8.5, the projected increase in Winter is 2.3, 3, and 3.8 °C; RCP 2.6 is 2.1, 2.5, and 2.5 °C during NF, MF, and FF, respectively. Also, during the Monsoon, the maximum temperature will vary from 1.3 °C during NF for RCP 2.6 to 3.2 °C during FF for RCP 8.5. Results show that the winter and monsoon seasons will be the most affected by the end of the 21st century.

3.4.3. *Minimum temperature*

The future changes in monthly minimum temperature according to RCP 2.6, 4.5 and 8.5 is represented in Figs. 4(c, f&i). The scenarios in the Near Future, Mid Future, and Far Future show that the minimum temperature will also increase almost every month except Mar and Apr of RCP 2.6 in all future periods, Mar of RCP 4.5 in NF and MF, and Mar and Apr of RCP 8.5 in NF only. The annual minimum temperature increases by 1.2-1.4 °C during NF, 1.3-2.2 °C for MF, and 1.3-3.6 °C during FF. Similar to the maximum temperature, the highest increment is observed for January in the case of the minimum temperature. Dec also shows a relatively higher increment as compared to other months. It is also noticed that with higher RCPs, the minimum temperature increases rapidly toward future periods. Moreover, a higher increase in minimum temperature during Jun-Jul and Dec-Jan indicates relatively warmer nights during Summers and Winters in the future compared to the base period.

Seasonal projection of minimum temperature also shows increased values in the three RCP in the future [Figs. 5(c, f&i)]. The maximum increase is projected for Winters, followed by the Monsoon and then Post-Monsoon, for all the RCPs in the future. The projected increase in Winter for RCP 8.5, is 2.6, 3.2 and 4.5 °C and for RCP 2.6 is 2.4, 2.5 and 2.7 °C during NF, MF and FF, respectively. Also, during the Monsoon, the minimum temperature will vary from 1.6 °C during NF for RCP 2.6 to 4.5 °C during FF for RCP 8.5. Results show that the winter and monsoon seasons will be the most affected, followed by the Post-Monsoon season at the end of the 21st century.

The present study uses the projections of CanESM2 and the results obtained are consistent with other such studies around the world. Several studies which uses CanESM2 projections have showed similar results over different parts of India (Menon *et al*., 2013, Shafiq *et al*., 2019, Vijayakumar *et al*., 2021). Global studies have also projected a hotter climate and wetter monsoon in future (Collins *et al*., 2013, Kitoh, 2017). The increase in temperature in future period may be attributed to the increasing concentration of Green House Gases, Aerosol, which may trap the heat into the atmosphere (Collins *et al*., 2013). Due to increased temperature, the water vapour content in the atmosphere will increase which may intensify the moisture extraction by the southwest monsoon leading to heavy rainfall in future at Sohra.

4. Conclusions

The future climate of Sohra was projected in terms of temperature and precipitation using the output of CanESM2. A statistical downscaling technique was used to downscale these outputs at the station level using SDSM 4.2. The daily data of maximum and minimum temperature and precipitation of Sohra for 1979-2020 was used to downscale the GCM outputs, and the period 1979-2005 was used for model calibration, while the period 2006-2020 was used for model validation. Sohra is a place with extreme climatic conditions, and downscaling of precipitation and temperature for this region is important for various impact studies on agriculture, tourism, and water resources.

The projection on precipitation reveals that the monthly precipitation will increase sufficiently from Apr to Jul and in Oct in the future under all RCPs. Also, the monthly maximum and minimum temperature will increase in future periods in all RCPs. The highest change in precipitation and maximum and minimum temperature are observed under RCP 8.5. The seasonal projection shows that the maximum increase in precipitation will be observed in the Monsoon from 266 mm for RCP 2.6 in NF to 1543 mm for RCP 8.5 in FF. Similarly, for maximum and minimum temperatures, the highest increment will be observed during the winter season as the increment in maximum and minimum temperatures will reach up to 3.8 and 4.5 °C under RCP 8.5 towards the end of the 21st century. Overall, the study suggests that in the future, precipitation will increase during the Monsoons, and the temperature extremes will increase during the winter season. It indicates that Sohra may witness a dry and harsh Winter as the precipitation change is negligible and the temperature change is highest during this season in future periods. Previous studies on climate extremes at Sohra also suggest that the Consecutive Dry Days (CDD) have increased significantly by 0.54 days/year, while the Consecutive Wet Days (CWD) have decreased significantly with 0.36 days/year during the recent period

1979-2020 (Kalita *et al.*, 2023). Therefore, water scarcity during the dry Winters may prevail in the future, which is a well-known problem for people living in Sohra (Mawroh and Husain, 2012; Mawroh, 2019). However, increase in Monsoon precipitation in the future may increase frequent flooding in low-lying areas such as the North-Eastern part of Bangladesh, as most of the rainwater from Sohra is drained into the Bangladesh flood plain during the Monsoon season.

The current study provides a basic representation of the future climate of Sohra using the ensemble mean of a single model output. However, there are uncertainties associated with the SDSM because it assumes the statistical relationship between the predictors and the predictions to be stationary at all future times. Also, using a single GCM output often leads to a biased estimation of future states. Further, uncertainties may arise due to the imperfect understanding of the physical process and feedback in the model. Therefore, the use of multi-model ensembles or multiple ensembles mean of single model can better represent the future climate. Moreover, downscaling from multiple GCMs with an RCM or from multiple RCMs could be a better alternative for reducing uncertainties. Hence, further study is recommended in this direction.

Acknowledgments

The authors are highly grateful to the Indian Meteorological Department and Cherrapunjee Holiday Resort for keeping track of the daily precipitation and temperature data of Sohra and for making it available publicly. Also, Atul Saxena (Principal Investigator) and Raju Kalita (Junior Research Fellow) are thankful to the Climate Change Programme Division, Department of Science and Technology, Govt. of India, for providing funds through a project (Sanction No. DST/CCP/HICAB/ SN-Meghalaya/177/2018(G)).

Disclaimer : The contents and views expressed in this study are the views of the authors and do not necessarily reflect the views of the organizations they belong to.

References

Akhtar, M., Ahmad, N. and Booij, M. J., 2008, "The impact of climate change on the water resources of Hindukush-Karakoru-Himalaya region under different glacier coverage scenarios", *J. hydrol.*, **355,** 1-4, 148-163. doi : https://doi:10.1016/j.jhydrol.2008.03.015.

Anandhi, A., Srinivas, V. V., Nanjundiah, R. S. and Nagesh Kumar D., 2007, "Downscaling precipitation to river basin in India for IPCC SRES scenarios using support vector machine", *Int. J. Climatol.*, **28**, 401-420. doi : https://doi:10.1002/joc.1529.

Asharaf, S. and Ahrens, B., 2015, "Indian summer monsoon rainfall processes in climate change scenarios", *J. Clim.*, **28,** 13, 5414-5429. doi : https://doi.org/10.1175/JCLI-D-14-00233.1.

Ashiq, M., Zhao, C., Ni, J. and Akhtar, M., 2010, "GIS-based high-resolution spatial interpolation of precipitation in mountain-plain areas of Upper Pakistan for regional climate change impact studies", *Theor. Appl. Climatol.*, **99,** 3, 239-253. doi : https://doi:10.1007/s00704-009-0140-y.

Basha, G., Kishore, P., Ratnam, M. V., Jayaraman, A., Kouchak, A. A., Ouarda, T. B. M. J. and Velicogna, I., 2017, "Historical and projected surface temperature over India during the 20th and 21st century", *Sci. Rep.*, **7**, 1, 1-10. doi : https://doi.org/10.1038/s41598-017-02130-3.

Bollasina, M. A., 2014, "Probing the monsoon pulse", *Nat. Clim. Change*, **4,** 6, 422-423. doi : https://doi.org/10.1038/nclimate2243.

Chaturvedi, R. K., Joshi, J., Jayaraman, M., Bala, G. and Ravindranath, N. H., 2012, "Multi-model climate change projections for India under representative concentration pathways", *Curr. Sci.*, **103**, 7, 791-802. doi : https://www.jstor.org/stable/24088836.

Collins, M., Knutti, R., Arblaster, J., Dufresne, J. D., Fichefet, T., Friedlingstein, P., Gao, X., Gutowski, W. J., Johns, T., Krinner, G., Shongwe, M., Tebaldi, C., Weaver, A. J. and Wehner, M., 2013, "Long-term Climate Change: Projections, Commitments and Irreversibility. Climate Change 2013: The Physical Science Basis. Contribution of Working Group I to the Fifth Assessment Report of the Intergovernmental Panel on Climate Change. Stocker, T. F., Qin, D., Plattner, G.-K., Tignor, M., Allen, S. K., Boschung, J., Nauels, A., Xia, Y., Bex, V. and Midgley P. M. (eds.), Cambridge University Press, Cambridge, UK and New York, USA, 1029-1120.

Das, J. and Umamahesh, N. V., 2022, "Heat wave magnitude over India under changing climate: Projections from CMIP5 and CMIP6 experiments", *Int. J. Climatol.*, **42**, 1, 331-351. doi : https://doi.org/10.1002/joc.7246.

Elshamy, M. E., Seierstad, I. A. and Sorteberg, A., 2009, "Impacts of climate change on Blue Nile flows using bias-corrected GCM scenarios", *Hydrol. Earth Syst. Sci.*, **13**, 551-565. doi : https://doi:10.5194/hess-13-551-2009.

Ghosh, S. and Mujumdar, P. P., 2008, "Statistical downscaling of GCM simulations to stream flow using relevance vector machine", *Ad. Water Resour.*, **31**, 132-146. doi : https://doi.org/10.1016/j.advwatres.2007.07.005.

Goyal, M. K. and Ojha, C. S. P., 2010, "Robust weighted regression as a downscaling tool in temperature projections", *Int. J. Glob. Warm.*, **2**, 3, 234-251. doi : https://doi:10.1504/IJGW.2010.036135.

Gusain, A., Ghosh, S. and Karmakar, S., 2020, "Added value of CMIP6 over CMIP5 models in simulating Indian summer monsoon rainfall", *Atmos. Res.*, **232**, 104680. doi : https://doi.org/10.1016/j.atmosres.2019.104680.

Huang, J., Zhang, J., Zhang, Z., Xu, C., Wang, B. and Yao, J., 2011, "Estimation of future precipitation change in the Yangtze River basin by using statistical downscaling method", *Stoch. Env. Res. Risk. A*, **25**, 6, 781-792. doi : https://doi:10.1007/s00477-010-0441-9.

IPCC, 2021, Climate Change 2021: The Physical Science Basis. Contribution of Working Group I to the Sixth Assessment

Report of the Intergovernmental Panel on Climate Change; Cambridge University Press, In press.

Kalita, R., Kalita, D. and Saxena, A., 2023, "Trends in extreme climate indices in Cherrapunji for the period 1979 to 2020", *J. Earth Syst. Sci.*, **132**, 74. doi : https://doi.org/10.1007/s12040-023-02087-0.

Kannan, S. and Ghosh, S., 2011, "Prediction of daily rainfall state in a river basin using statistical downscaling from GCM output", *Stoch. Env. Res. Risk. A*, **25**, 4, 457-474. doi : https://doi:10.1007/s00477-010-0415-y.

Khadka, D. and Pathak, D., 2016, "Climate change projection for the marsyangdi river basin, Nepal using statistical downscaling of GCM and its implications in geodisasters", *Geo. Disas.*, **3**, 1, 1-15. doi : https://doi.org/10.1186/s40677-016-0050-0.

Kitoh, A., 2017 "The Asian monsoon and its future change in climate models: A review", *J. Meteorol. Soc. Japan.* Ser. II, **95**, 1, 7-33.

Kumar, P., Wiltshire, A., Mathison, C., Asharaf, S., Ahrens, B., Lucas-Picher, P., Christensen, J.H., Gobiet, A., Saeed, F., Hagemann, S. and Jacob, D., 2013, "Downscaled climate change projections with uncertainty assessment over India using a high resolution multi-model approach", *Sci. Total Environ.*,**468**, S18-S30. doi : http://dx.doi.org/10.1016/j.scitotenv.2013.01.051.

Lee, J.Y. and Wang, B., 2014, "Future change of global Monsoon in the CMIP5", *Clim. Dyn.*, **42**, 1, 101-119. doi : https://doi.org/10.1007/s00382-012-1564-0.

Mahmood, R. and Babel, M. S., 2013, "Evaluation of SDSM developed by annual and monthly sub-models for downscaling temperature and precipitation in the Jhelum basin, Pakistan and India", *Theor. Appl. Climatol.*, **113**,1, 27-44. doi : https://doi.org/10.1007/s00704-012-0765-0.

Maraun, D., Wetterhall, F., Ireson, A. M., Chandler, R. E., Kendon, E. J., Widmann, M., Brienen, S., Rust, H. W., Sauter, T., Themeßl, M. and Venema, V. K. C., 2010, "Precipitation downscaling under climate change: Recent developments to bridge the gap between dynamical models and the end user", *Rev. Geophys.*, **48**, RG3003. doi : https://doi:10.1029/2009RG000314.

Mawroh, B. and Husain, Z., 2012, "Scarcity of water for domestic consumption in Cherrapunjee", *in: Husain, Z. and Cajee, L. (Eds.), Water Crisis in the Indian Subcontinent*, Bookwell & North-Eastern Hill University, Shillong, 467-486.

Mawroh, B., 2019, "Water scarcity in Sohra (Cherrapunjee): A paradox", *Transient*, **8**, 40-49. https://donboscocollege.ac.in/public/uploads/filemanager/Transient%20VIII%20upload.pdf#page=52.

Mei, R., Ashfaq, M., Rastogi, D., Leung, L.R. and Dominguez, F., 2015, "Dominating controls for wetter South Asian summer monsoon in the twenty-first century", *J. Clim.*, **28**, 8, 3400-3419. doi : https://doi.org/10.1175/JCLI-D-14-00355.1.

Menon, A., Levermann, A., Schewe, J., Lehmann, J. and Frieler, K., 2013, "Consistent increase in Indian monsoon rainfall and its variability across CMIP-5 models", *Earth. Syst. Dyn.*,**4**, 2, 287-300. doi : https://doi.org/10.5194/esd-4-287-2013.

Salvi, K. and Ghosh, S., 2013, "High-resolution multisite daily rainfall projections in India with statistical downscaling for climate change impacts assessment", *J. Geophys. Res.*, **118**, 9, 3557-3578. doi : https://doi.org/10.1002/jgrd.50280.

Shafiq, M. u., Ramzan, S., Ahmed, P. and Dimri, A. P., 2019, "Assessment of present and future climate change over Kashmir Himalayas, India", *Theor. Appl. Climatol*, **137**, 3183-3195. doi : https://doi.org/10.1007/s00704-019-02807-x.

Sharma, D., Das Gupta, A. and Babel, M. S., 2007, "Spatial disaggregation of bias-corrected GCM precipitation for improved hydrologic simulation: Ping River Basin, Thailand", *Hydrol. Earth Syst. Sci.*, **4**, 35-74. doi : https://doi.org/10.5194/hess-11-1373-2007.

Sharmila, S., Joseph, S., Sahai, A. K., Abhilash, S. and Chattopadhyay, R., 2015, "Future projection of Indian summer monsoon variability under climate change scenario: An assessment from CMIP5 climate models", *Glob. Planet. Change*, **124**, 62-78. doi : https://doi.org/10.1016/j.gloplacha.2014.11.004.

Souvignet, M. and Heinrich, J., 2011, "Statistical downscaling in the arid central Andes: uncertainty analysis of multi-model simulated temperature and precipitation", *Theor. Appl. Climatol.*, **106**, 1, 229-244. doi : https://doi:10.1007/s00704-011-0430-z.

Tripathi, S., Srinivas, V. V. and Nanjundiah, R. S., 2006, "Downscaling of precipitation for climate change scenarios: a support vector machine approach", *J. Hydrol.*, **330**, 3-4, 621-640. doi : https://doi:10.1016/j.jhydrol.2006.04.030.

Varghese, S. J., Surendran, S., Rajendran, K. and Kitoh, A., 2020, "Future projections of Indian Summer Monsoon under multiple RCPs using a high resolution global climate model multiforcing ensemble simulations", *Clim. Dyn.*, **54**, 3, 1315-1328. doi : https://doi.org/10.1007/s00382-019-05059-7.

Vijayakumar, S., Nayak, A. K., Ramaraj, A. P., Swain, C. K., Geethalakshmi, V., Pazhanivelan, S., Tripathi, R. and Sudarmanian, N. S., 2021, "Rainfall and temperature projections and their impact assessment using CMIP5 models under different RCP scenarios for the eastern coastal region of India" *Curr. Sci.*, **121**,2, 222.

Wetterhall, F., Bárdossy, A., Chen, D., Halldin, S. and Xu, C. Y., 2009, "Statistical downscaling of daily precipitation over Sweden using GCM output", *Theor. Appl. Climatol.*, **96**, 1, 95-103. doi : https://doi:10.1007/s00704-008-0038-0.

Wilby, R. L., Dawson, C. W. and Barrow, E. M., 2002, "SDSM-a decision support tool for the assessment of regional climate change impacts", *Environ. Model. Softw.*, **17**, 2, 145-157. doi : https://doi.org/10.1016/S1364-8152(01)00060-3.